Solid Polymer Single-Ion Conductors: Synthesis and Properties

Lyudmila M. Bronstein,*,† Robert L. Karlinsey,‡ Barry Stein,§ Zheng Yi,|| John Carini,|| and Josef W. Zwanziger⊥

Departments of Chemistry, Biology, and Physics, Indiana University, Bloomington, Indiana 47405, Indiana University School of Dentistry, Oral Health Research Institute, Indianapolis, Indiana 46202, and Department of Chemistry and Institute for Research in Materials, Dalhousie University, Halifax, Nova Scotia, Canada B3H 4J3

Received October 3, 2005. Revised Manuscript Received November 28, 2005

Optimal battery electrolyte materials provide for high transport of a single ionic species. Here we report solid single-ion conductors (SICs) based on composite polymer electrolytes consisting of poly(ethylene glycol) (PEG) and an organic−inorganic component (OIC) formed in situ. The resulting solid films showed transport properties with conductivity as high as 10^{-4} S/cm at room temperature and a cation transference number of 0.9. The materials were characterized using solid-state NMR, differential scanning calorimetry, X-ray diffraction, transmission electron microscopy (TEM), and impedance spectroscopy. The OIC was formed by sol−gel reaction of the three precursors: the sodium salt of 3-trihydroxysilylpropylmethylphosphonate (SPMP), (3-glycidylopropyl)trimethoxysilane (GLYMO), and tetramethoxysilane, resulting in a high degree of three-dimensional network character of OIC within SIC solid polymer electrolytes as indicated by solid-state NMR. TEM examination of calcined OIC shows that the silicate particles are fairly uniform and measure approximately 15 nm in diameter. Their uniformity and small size lead to the homogeneity of the composite material. The glycidyl group of GLYMO enhances the compatibility of OIC with PEG. The phosphonate group of SPMP furnishes immobile anions, while Na^+ cations are the only source of conductivity.

Introduction

Solid polymer electrolytes (SPEs) for secondary Li batteries continue to be a topic of increased interest due to their potential advantages, including safety and ease of packaging and containment compared to liquid or gellike electrolytes. Recently, composite SPEs made of an inorganic component along with a conventional salt-in-polymer electrolyte have received considerable attention due to suppression of poly(ethylene oxide) (PEO) crystallization, enhancement of the mechanical properties, and, often, enhancement of conductivity and Li transference numbers.[1−18] All these parameters are important for successful application of these SPEs in secondary lithium batteries. Composite polymer electrolytes can be prepared in two different ways: (i) inorganic fillers (TiO_2, Al_2O_3, and SiO_2, etc.)[2,9−11,16−25] or clay platelets can be incorporated in polymers[26−29] or (ii) metal oxides can be

* To whom correspondence should be addressed. E-mail: lybronst@indiana.edu.
† Department of Chemistry, Indiana University.
‡ Oral Health Research Institute.
§ Department of Biology, Indiana University.
|| Department of Physics, Indiana University.
⊥ Dalhousie University.

(1) Scrosati, B. *Nature* **1995**, *373* (6515), 557−558.
(2) Nookala, M.; Kumar, B.; Rodrigues, S. *J. Power Sources* **2002**, *111*, 165−172.
(3) Wang, C.; Xia, Y.; Koumoto, K.; Sakai, T. *J. Electrochem. Soc.* **2002**, *149*, A967−A972.
(4) Persi, L.; Croce, F.; Scrosati, B.; Plichta, E.; Hendrickson, M. A. *J. Electrochem. Soc* **2002**, *149*, A212−A216.
(5) Li, Q.; Imanishi, N.; Takeda, Y.; Hirano, A.; Yamamoto, O. *Ionics* **2002**, *8*, 79−84.
(6) Digar, M.; Hung, S.-L.; Wen, T.-C. *J. Appl. Polym. Sci.* **2001**, *80*, 1319−1328.
(7) Wieczorek, W.; Lipka, P.; Zukowska, G.; Wycislik, H. *J. Phys. Chem. B* **1998**, *102*, 6968−6974.
(8) Best, A. S.; Adebahr, J.; Jacobsson, P.; MacFarlane, D. R.; Forsyth, M. *Macromolecules* **2001**, *34*, 4549−4555.
(9) Marcinek, M.; Bac, A.; Lipka, P.; Zalewska, A.; Zukowska, G.; Borkowska, R.; Wieczorek, W. *J. Phys. Chem. B* **2000**, *104*, 11088−11093.
(10) Adebahr, J.; Best, A. S.; Byrne, N.; Jacobsson, P.; MacFarlane, D. R.; Forsyth, M. *Phys. Chem. Chem. Phys.* **2003**, *5*, 720−725.
(11) Cheung, I. W.; Chin, K. B.; Greene, E. R.; Smart, M. C.; Abbrent, S.; Greenbaum, S. G.; Prakash, G. K. S.; Surampudi, S. *Electrochim. Acta* **2003**, *48*, 2149−2156.
(12) Meyer, W. H. *Adv. Mater.* **1998**, *10*, 439−448.
(13) Sadoway, D. R.; Huang, B. Y.; Trapa, P. E.; Soo, P. P.; Bannerjee, P.; Mayes, A. M. *J. Power Sources* **2001**, *97−98*, 621−623.
(14) Soo, P. P.; Huang, B. Y.; Jang, Y. I.; Chiang, Y. M.; Sadoway, D. R.; Mayes, A. M. *J. Electrochem. Soc.* **1999**, *146*, 32−37.
(15) Capiglia, C.; Mustarelli, P.; Quartarone, E.; Tomasi, C.; Magistris, A. *Solid State Ionics* **1999**, *118*, 73−79.
(16) Kumar, B.; Rodrigues, S. J.; Scanlon, L. G. *J. Electrochem. Soc.* **2001**, *148*, A1191−A1195.
(17) Morita, M.; Fujisaki, T.; Yoshimoto, N.; Ishikawa, M. *Electrochim. Acta* **2001**, *46*, 1565−1569.
(18) Sun, H. Y.; Sohn, H.-J.; Yamamoto, O.; Takeda, Y.; Imanishi, N. *J. Electrochem. Soc.* **1999**, *146*, 1672−1676.
(19) Bloise, A. C.; Tambelli, C. C.; Franco, R. W. A.; Donoso, J. P.; Magon, C. J.; Souza, M. F.; Rosario, A. V.; Pereira, E. C. *Electrochim. Acta* **2001**, *46*, 1571−1579.
(20) Croce, F.; Persi, L.; Scrosati, B.; Serraino-Fiory, F.; Plichta, E.; Hendrickson, M. A. *Electrochim. Acta* **2001**, *46*, 2457−2461.
(21) Scrosati, B.; Croce, F.; Panero, S. *J. Power Sources* **2001**, *100*, 93−100.
(22) Weston, J. E.; Steele, B. C. H. *Solid State Ionics* **1982**, *7*, 75−79.
(23) Croce, F.; Appetecchi, G. B.; Persi, L.; Scrosati, B. *Nature* **1998**, *394* (6692), 456−458.
(24) Wieczorek, W.; Stevens, J. R.; Florjanczyk, Z. *Solid State Ionics* **1996**, *85*, 67−72.
(25) Tambelli, C. C.; Bloise, A. C.; Rosario, A. V.; Pereira, E. C.; Magon, C. J.; Donoso, J. P. *Electrochim. Acta* **2002**, *47*, 1677−1682.
(26) Vaia, R. A.; Vasudevan, S.; Krawiec, W.; Scanlon, L. G.; Giannelis, E. P. *Adv. Mater.* **1995**, *7*, 154−156.

10.1021/cm052195l CCC: $33.50
Published on Web 01/10/2006

formed within a polymeric system, thus providing fresh interfaces between inorganic and polymer components and potentially enhanced properties. In situ formation of the inorganic component can result in nanoparticles or interpenetrating networks (or both),[30−32] while the morphology of the inorganic component depends on its fraction and on the reaction conditions. Either physical sorption[33] or chemical bonding[30,31,34] can provide interaction between organic and inorganic components of SPEs. In our recent publications we described a series of composite polymer electrolytes consisting of PEO, lithium triflate, and an organically modified organic−inorganic component (OIC) made of aluminosilicate or silicate particles and prepared in situ.[31,35−38] High room-temperature conductivity (about 10^{-4} S/cm) was recently reported for novel network-type SPEs, resembling composite materials due to cross-linking of pentamethylcyclopentasiloxanes with PEO moieties.[39]

Unfortunately, in the majority of SPEs, including composite materials, the ion mobility is not dominated by that of single cations but rather by the motion of ion aggregates of various sizes. In other words the transference number for the cations can be much less than unity. Low transference numbers are particularly serious in battery applications, because the mobile anion will quickly form an impenetrable polarizing layer at the cathode. Therefore recharging the cell requires more energy, time and a larger electrochemical potential.[40] Polymer−inorganic intercalate materials combine advantages of composite materials and provide a single-ion conducting mechanism due to fixed anion sites and therefore a high transference number for the cations. Such intercalates have been made with both the PEO or PEO-based polymers[29,41,42] and polyphosphazenes;[43] a problem with this approach is often low conductivity (below 10^{-5} S/cm at room temperature) and the anisotropy of the resulting conductivity.

It is possible to exclude anion transport in noncomposite SPEs by attaching the anions as pendant groups to the mobile polymer or to use mixtures of PEO-containing polymers and polyelectrolytes.[40,44−47] In the latter case, however, the miscibility of two polymers is often problematic. The siloxyaluminate polymers synthesized by Shriver and colleagues represent a potentially major improvement on this approach since they are isotropic materials showing relatively high conductivity at room temperature (about 10^{-5} S/cm) and a weak dependence of conductivity on temperature.[48,49] They are, however, relatively complex to synthesize.

In this paper we report a robust method for preparation of single-ion conducting composite polymer electrolytes in a one-pot reaction procedure. This is performed by tethering the anion directly to the inorganic component of the SPE using a silane with the sodium phosphonate group, while poly(ethylene glycol) (PEG) granting a cation transfer is salt-free. This method leads to a new type of single-ion conductors with high conductivities and cation transference numbers. The structure and electrochemical properties of these SICs are described using solid-state NMR, differential scanning calorimetry (DSC), X-ray diffraction (XRD), transmission electron microscopy (TEM), and electrochemical measurements.

Experimental Section

Materials. The sodium salt of 3-trihydroxysilylpropylmethylphosphonate (SPMP, 42% in water, Gelest), (3-glycidoxypropyl)trimethoxysilane (GLYMO, Fluka), tetramethoxysilane (TMOS, Aldrich), poly(ethylene glycol) with a molecular weight of 600 (PEG, Aldrich), and methanol (EM Industries, Inc.) were used without further purification.

Synthesis. The OIC part of the composite was prepared by a sol−gel reaction of a mixture of TMOS, GLYMO, and SPMP in a solution of PEG in methanol. Molar ratios and other conditions are presented in Table 1. In a typical experiment a vial with a stir bar was charged with 0.509 g of PEG (45 wt % total composite) and 2 mL of methanol. After the polymer dissolution, 0.1065 g (0.7 mmol) of TMOS, 0.4135 g (1.75 mmol) of GLYMO, and 0.595 g of 42% solution of SPMP (1.05 mmol) in water were added and the reaction solution was stirred for a predetermined amount of time (see Table 1) while hydrolysis and initial condensation took place. Afterward the reaction solution was spun on a Teflon dish and heated at 60 °C for 2 h for evaporation of solvent and OIC condensation. The solid film was treated at 130 °C in a vacuum for 1 h to complete condensation. Films were cooled in a desiccator and then easily removed from the dish. Samples were sealed and kept in a desiccator. Additionally, some samples were dried before

(27) Sandi, G.; Carrado, K. A.; Joachin, H.; Lu, W.; Prakash, J. *J. Power Sources* **2003**, *119−121*, 492−496.
(28) Chen, H.-W.; Chiu, C.-Y.; Wu, H.-D.; Shen, I.-W.; Chang, F.-C. *Polymer* **2002**, *43*, 5011−5016.
(29) Kurian, M.; Galvin, M. E.; Trapa, P. E.; Sadoway, D. R.; Mayes, A. M. *Electrochim. Acta* **2005**, *50*, 2125−2134.
(30) Popall, M.; Andrei, M.; Kappel, J.; Kron, J.; Olma, K.; Olsowski, B. *Electrochim. Acta* **1998**, *43*, 1155−1161.
(31) Bronstein, L. M.; Joo, C.; Karlinsey, R.; Ryder, A.; Zwanziger, J. W. *Chem. Mater.* **2001**, *13*, 3678−3684.
(32) Kao, H.-M.; Chen, C.-L. *Angew. Chem., Int. Ed.* **2004**, *43*, 980−984.
(33) Jiang, S.; Yu, D.; Ji, X.; An, L.; Jiang, B. *Polymer* **2000**, *41*, 2041−2046.
(34) Di Noto, V.; Zago, V.; Biscazzo, S.; Vittadello, M. *Electrochim. Acta* **2003**, *48*, 541−554.
(35) Bronstein, L. M.; Karlinsey, R. L.; Ritter, K.; Joo, C.-G.; Stein, B.; Zwanziger, J. W. *J. Mater. Chem.* **2004**, *14*, 1812−1820.
(36) Bronstein, L. M.; Karlinsey, R.; Stein, B.; Zwanziger, J. W. *Solid State Ionics* **2005**, *176*, 559−570.
(37) Bronstein, L. M.; Ashcraft, E.; DeSanto, P., Jr.; Karlinsey, R. L.; Zwanziger, J. W. *J. Phys. Chem. B* **2004**, *108*, 5851−5858.
(38) Karlinsey, R. L.; Bronstein, L. M.; Zwanziger, J. W. *J. Phys. Chem. B.* **2004**, *108*, 918−928.
(39) Zhang, Z.; Lyons, L. J.; Amine, K.; West, R. *Macromolecules* **2005**, *38*, 5714−5720.
(40) Mandal, B. K.; Walsh, C. J.; Sooksimuang, T.; Behroozi, S. J.; Kim, S.-G.; Kim, Y.-T.; Smotkin, E. S.; Filler, R.; Castro, C. *Chem. Mater.* **2000**, *12*, 6−8.
(41) Giannelis, E. P. *Adv. Mater.* **1996**, *8*, 29−35.
(42) Lemmon, J. P.; Wu, J.; Oriakhi, C.; Lerner, M. M. *Electrochim. Acta* **1995**, *40*, 2245−2249.
(43) Hutchison, J. C.; Bissessur, R.; Shriver, D. F. *Chem. Mater.* **1996**, *8*, 1597−1599.
(44) Tsutsumi, H.; Yamamoto, M.; Morita, M.; Matsuda, Y.; Nakamura, T.; Asai, H. *J. Power Sources* **1993**, *41*, 291−298.
(45) Bayoudh, S.; Parizel, N.; Reibel, L. *Polym. Int.* **2000**, *49*, 703−711.
(46) Hardy, L. C.; Shriver, D. F. *J. Am. Chem. Soc.* **1985**, *107*, 7, 3823−3828.
(47) Watanabe, M.; Suzuki, Y.; Nishimoto, A. *Electrochim. Acta* **2000**, *45*, 1187−1192.
(48) Rawsky, G. C.; Fujinami, T.; Shriver, D. F. *Chem. Mater.* **1994**, *6*, 2208−2209.
(49) Fujinami, T.; Tokimun, A.; Mehta, M. A.; Shriver, D. F.; Rawsky, G. C. *Chem. Mater.* **1997**, *9*, 2236−2239.

Table 1. Preparation Conditions and Characteristics of Single-Ion Conducting SPEs Based on 600 MW PEG and OIC Derived from TMOS, GLYMO, and SPMP

sample notation	TMOS:GLYMO:SPMP ratio	PEG:Na ratio	methanol vol, mL	reacn time, h	conductivity, S cm^{-1}	T_g, °C	T_{crys} (center of gravity)	T_m (center of gravity)	transf no.
T-G-S-PEG-1-1	1:2.5:1.5	11:1	2.0	1	9.77×10^{-6}	−70	−47	1	0.7
T-G-S-PEG-1-2	1:2.5:1.5	11:1	2.0	1.75[a]	5.53×10^{-6}	−70	−46	3	0.7
T-G-S-PEG-1-3	1:2.5:1.5	11:1	1.5	1.5	9.45×10^{-6}	−70	−49	3	0.7
T-G-S-PEG-2	1:2.9:1.2	14:1	1.5	1.5	6.94×10^{-6}	−70	−48	3	0.7
T-G-S-PEG-3-1	1:2.9:1.3	12.8:1	1.5	1.5	9.69×10^{-6}	−71	−48	1	0.7
T-G-S-PEG-3-1, dried at 30 °C for 24 h	1:2.9:1.3	12.8:1	1.5	1.5	9.13×10^{-5}	−71	−48	2	0.9
T-G-S-PEG-3-2	1:2.9:1.3	12.8:1	1.5	2.0[a]	6.20×10^{-6}	−70	−49	3	0.6
T-G-S-PEG-3-3	1:2.9:1.3	12.8:1	2.0	1.5		−70	−48	4	0.7
T-G-S-PEG-3-3, dried at 30 °C for 24 h	1:2.9:1.3	12.8:1	2.0	1.5	9.75×10^{-5}	−70	−48	3	0.9

[a] Reaction was carried out until reaction solution became turbid (condensation progressed).

measurements at 30 °C in a vacuum oven. Notation T-G-S-PEG used in this paper stands for the composite based on TMOS, GLYMO, SPMP, and PEG.

Calcination was carried out at 500 °C for 4 h in nitrogen and for 12 h in oxygen.

Characterization. Samples for TEM were prepared by grinding the calcined samples using a mortar and pestle followed by suspension in acetone. A drop of the sample suspension was placed onto a carbon-coated copper grid. The acetone was then evaporated off at room temperature. Images were acquired at an accelerating voltage of 100 kV on a JEOL JEM1010 microscope.

DSC was performed with Perkin-Elmer DSC 7 and Q10 TA Instruments calorimeters. Sample masses varied from 5 to 20 mg, and the samples were hermetically sealed in aluminum pans. Samples were scanned between −100 and +100 °C at a rate of 10 °C/min, using liquid nitrogen as coolant. Glass transition regions were then determined using the fictive temperature method. Both indium and cyclohexane were used to reference thermal events. Melting points and associated enthalpies were analyzed by deconvolution since observed endothermic transitions were not symmetric. The melting points reflect the center of gravity melting, and the tabulated enthalpy is the sum of the peak-fit areas.

Solid-state ^{29}Si and ^{13}C magic angle spinning (MAS) NMR was performed using a Bruker Avance DSX spectrometer. Spectra were obtained using a 4 mm MAS probe with the spin rate locked at 10 kHz. Due to the low sensitivity of ^{13}C and ^{29}Si, cross-polarization (CP) from protons was employed to improve the signal. The ^{1}H $\pi/2$ pulse length was about 5.5 μs, and the CP contact time was about 1000 μs for carbon and silicon, respectively. The recycle time was between 3 and 4 s. The carbon and silicon spectra were referenced to glycine and kaolin, respectively. Peak analysis of the silicon environments was performed by fitting Gaussians to the NMR line shapes.

AC admittance spectroscopy was used to measure conductivity and dielectric constants of cast films. To obtain excellent electrode−electrolyte contact, gold electrodes of a known area (0.0647 cm^2) were directly attached to the film by sputter coating, using a Polaron E5100 sputter coater. Films were placed in a home-built temperature-controlled cell for measurements using a HP 4192A impedance analyzer and a Quantum Design digital RG bridge (Model 1802, to measure and control the cell temperature). After sputtering, the films were held at room temperature for several days while their admittance was monitored, since, as described below, we observe that the bulk conductivity relaxes over time after the samples have been heated above 60 °C and then cooled to room temperature.

The admittance response of the material was measured in two ways. At a fixed or controlled temperature, data were collected by sweeping the frequencies from 5 Hz to 10 MHz with a 1 V signal (to improve the response from thick films). Bulk conductances were then extrapolated by modeling the admittance of the sample at medium to high frequencies. Alternately, during continuous heating, cooling, or annealing runs, the frequency was kept fixed at 50 kHz and the conductance value at that frequency was used as the bulk value (this agrees within 20% of the value obtained from modeling the frequency response). Both silicon and $(PEO)_{14}LiO_3SCF_3$ were used as reference materials for conductivity. Dielectric constants were obtained by taking the minimum in a capacitance versus frequency curve. Pure PEO ($\epsilon_r \sim 5$)[50] was used as a reference material.

Variable-temperature (VT) conductivity measurements were carried out using the following protocol. First room-temperature conductivity of the sample was measured using the HP impedance analyzer. Then the sample was cooled to −50 °C, while the sample admittance was continuously measured at 50 kHz. After that the sample was warmed in 10 deg steps back to room temperature, measuring the ac admittance from 5 Hz to 10 MHz at −50, −40, ..., 20 °C. Then the sample was warmed from room temperature to 80 °C in 10 deg steps, measuring the ac admittance from 5 Hz to 10 MHz at 30, 40, ..., 80 °C. At this point the conductivity is in a nearly "as delivered" state from −50 to +80 °C. The sample was held at 80 °C for several hours while the sample admittance was measured continuously at 50 kHz (until the conductivity stops decreasing). Then the sample was cooled back to room temperature, and the sample admittance at 50 kHz was measured continuously. Finally, the sample was held for 4 days at room temperature and conductivity was measured.

Transference numbers were determined from slight modification of the popular steady-state method, which entails polarizing a symmetric polymer electrolyte cell galvano-

(50) McCrum, N. G.; Read, B. E.; Williams, G. *Inelastic and Dielectric Effects in Polymeric Solids*; Dover: New York, 1967.

statically and assumes complete dissociation of the salt.[51] Lithium foil (0.25 mm thick) was used as the electrodes. The electrochemical cell assembled in a glovebox was placed inside a positive-pressure chamber purged with Ar during the experiment. Polarization was assumed complete when the measured voltage reading leveled off during constant current charging to the cell (between 1 and 100 μA). Once polarized the current source was cut and the corresponding voltage was recorded over a period of 24 h. Typically for electrolytes, the decay curve does not produce a clear single relaxation due to the contributions of various charged species present in the material (including positive, negative, and associated species); therefore, several diffusion coefficients can be estimated. Cation transference numbers are then approximated by considering the fraction of cations diffusing through the electrolyte. The solid polymer system, PEO + LiI, was used as a reference electrolyte with the estimated lithium transference number (0.4) in reasonable agreement with published results (0.3).[52] Our results also agree with those based on the analogous system made by colleagues in another laboratory.[53]

When the observed voltage decay curve does not reflect a single relaxation process, the relaxation profile is split into two distinct regions with each one corresponding to either sodium ion or hydrated sodium ion relaxation. This enabled diffusion coefficients of each species to be estimated; subsequently, the cation transference number was then calculated by taking the fraction of the sodium diffusing through the electrolyte. "PEO + LiI" was used as a reference electrolyte with the lithium transference number (0.4) in reasonable agreement with published results (0.3).[52]

Results and Discussion

Synthesis and Structure: NMR. For development of composite single-ion SPEs, we used a general approach explored by us and others earlier, i.e., formation of OIC particles in situ in polymeric phase using a sol−gel reaction. But unlike earlier works, here we used a silane, SPMP, bearing a tethered anion and a potentially mobile cation (Na^+). To enhance formation of the 3D silicate network, we also chose TMOS as a reagent and attempted synthesis of a composite whose OIC contained TMOS and SPMP at a molar ratio of 1 to 4. Since the pH of the SPMP aqueous solution is 12.0, no pH adjustment was necessary to initiate a sol−gel reaction. We screened three solvents: tetrahydrofuran, chloroform, and methanol, for compatibility of all reagents and found out that in methanol this mixture gives a homogeneous solution with PEG. However, the system phase separates when a film is formed, indicating poor miscibility between this silicate and PEG. To enhance compatibility of PEG with OIC, we employed partial replacement of SPMP with GLYMO. As was reported earlier,[31,36,54,55] the glycidyl group of GLYMO increases miscibility of the inorganic phase with PEG, preventing macroseparation of the organic phase from the OIC: this group can be polymerized in the presence of certain additives (for example, Al tri-*sec*-butoxide), giving oligo(ethylene oxide) chains,[56] and may react with terminal hydroxyl groups of PEG, which results in additional cross-linking within SPE.[57]

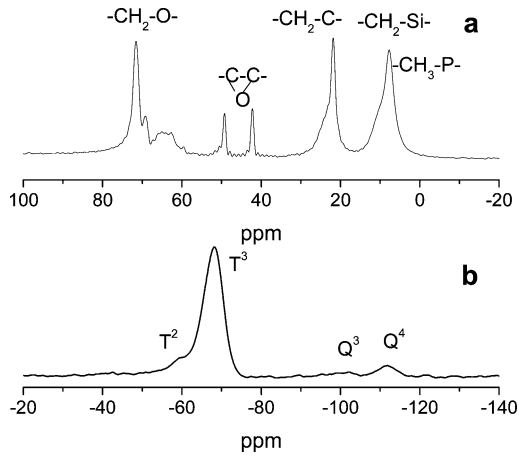

Figure 1. ^{13}C (a) and ^{29}Si (b) NMR spectra of T-G-S-PEG-3-1.

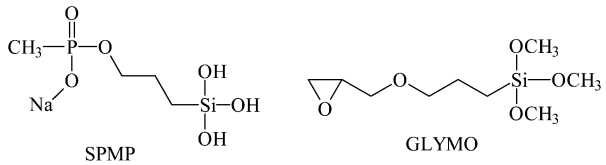

We varied the composition of the materials and studied the influence of reaction conditions such as the reagent molar ratio and concentration, the PEG content, and the reaction time on structure and electrochemical properties of the composite SPEs (Table 1). The local structure of the composite materials was studied with solid-state NMR. The carbon and silicon CP MAS spectra are shown in Figure 1 for a representative composition: T-G-S-PEG-3-1 (see Table 1 for details). Other compositions show similar spectra. The carbon spectrum shows resonances, assigned to -C−O- linkages in different precursors (71, 69, and ∼65 ppm), a glycidyl group (49 and 42 ppm), $-CH_2-$ groups (22 ppm), -C−Si- and CH_3-P units (8 ppm). The assignment of the resonances was carried out using a comparison with the published data[31,54,56] and simulation with ACD/CNMR software.[58] All these groups are possible on the basis of the structure of the precursors, but not all of them should necessarily be present. For example, the presence of two strong signals attributed to glycidyl groups reveals that these groups are very stable in the reaction conditions similar to the composite materials based solely on GLYMO and TMOS.[36] Conversely, when the OIC contains some amount of aluminum tri-*sec*-butoxide, glycidyl groups are fully

(51) Bruce, P. G.; Vincent, C. A. *Faraday Discuss. Chem. Soc.* **1989**, *88*, 43−54.
(52) Bouridah, A.; Dalard, F.; Deroo, D.; Armand, M. B. *Solid State Ionics* **1986**, *18 and 19*, 287−290.
(53) Ulrich, R.; Zwanziger, J. W.; De Paul, S. M.; Reiche, A.; Leuninger, H.; Spies, H. W.; Wiesner, U. *Adv. Mater.* **2002**, *14*, 1134−1137.
(54) Templin, M.; Franck, A.; Du Chesne, A.; Leist, H.; Zhang, Y.; Ulrich, R.; Schadler, V.; Wiesner, U. *Science* **1997**, *278*, 1795−1798.
(55) Popall, M.; Durand, H. *Electrochim. Acta* **1992**, *37*, 1593−1597.
(56) Templin, M.; Wiesner, U.; Spies, H. W. *Adv. Mater.* **1997**, *9*, 814−817.
(57) Ulrich, R.; Zwanziger, J. W.; De Paul, S. M.; Richert, R.; Wiesner, U.; Spiess, H. W. *Polym. Mater. Sci. Eng.* **1999**, *80*, 610−611.
(58) http://www.acdlabs.com/products/spec_lab/predict_nmr/cnmr/

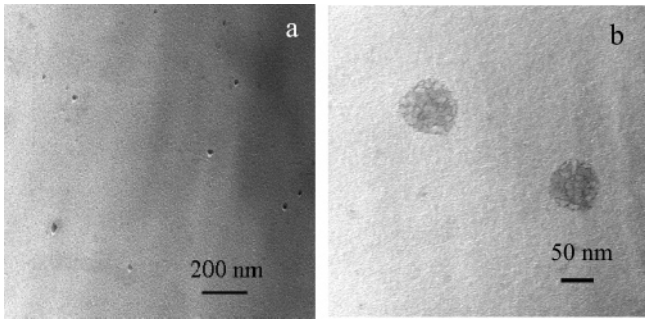

Figure 2. TEM images of the silicates obtained after calcination of T-G-S-PEG-3-1 (a) and T-G-S-PEG-3-2 (b).

reacted.[31,36,54,56] On the other hand, we found that the addition of GLYMO improves mechanical properties of the composite SIC films; thus, one might presume that some fraction of GLYMO glycidyl groups reacted with OH groups of PEG, providing cross-linking between PEG and OIC.[57] However solid-state NMR data do not allow quantitative assessment of the fraction of the glycidyl groups reacted.

The ^{29}Si CP MAS NMR spectrum of T-G-S-PEG-3-1 contains four signals: T^2 {C−SiO_2(OH)}, T^3 {C−SiO_3}, Q^3 {SiO_3(OH)}, and Q^4 {SiO_4}, yet T^2 and Q^3 signals are very weak, while T^3 and Q^4 dominate the spectrum. This indicates a high degree of three-dimensional network character of OIC within SIC SPEs. It is noteworthy that SPMP contains silanol groups which are stable in aqueous solution for months (this silane is supplied as a 42% solution in water), while they easily react with methoxy groups of TMOS and GLYMO in the reaction solution. It was observed that, depending on the reaction conditions, a reaction time of only 1.5−2 h may result in the formation of turbid solution, indicating the presence of gel silicate particles. As discussed below, however, in the majority of experiments, we carried out our reaction prior to a "cloud point" (gel formation) since it resulted in SIC films with better electrochemical performance.

Structure and Mobility: TEM, DSC, and XRD. As suggested in our preceding papers,[36,37] one of the ways to characterize the composite SPEs is to evaluate the size and shape of silicate or aluminosilicate domains. To accomplish that, we used calcination of SPE films at 500 °C for 4 h in nitrogen and 12 h in air, resulting in the removal of organic matter while the inorganic component retains its size and shape, imitating the structure of silicate domains in SPE. This approach is based on the well-established fact that the structure of mesoporous materials cast over block copolymer templates replicates the structure of the block copolymer template.[59,60] Examples of preservation of the template structure after calcination were also reported in refs 61 and 62. Figure 2a shows the TEM image of the calcined T-G-S-PEG-3-1 (Table 1). One can see that silicate particles are

Scheme 1. Schematic Representation of Composite SIC

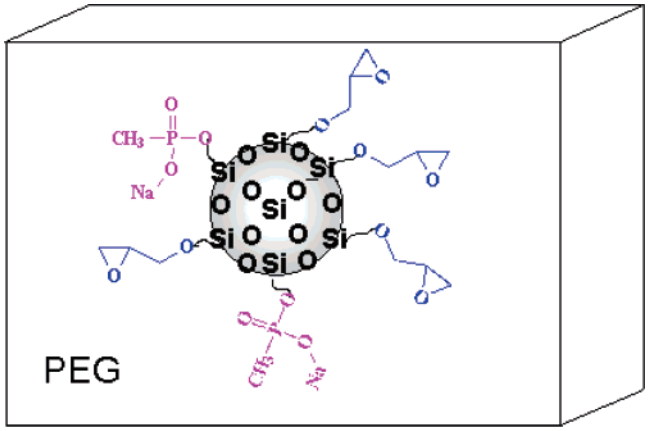

fairly uniform and measure approximately 15 nm in diameter. Their uniformity and small size should prevent heterogeneity of the material, observed by us earlier for composite materials containing aluminosilicate OIC.[36] The TEM and NMR data allow us to depict the composite SIC as shown in Scheme 1.

The electrochemical properties of SPEs are determined by the mobility of cations (the latter are normally related to polymer mobility) and by interaction of cations with anions. In the present material the anions are relatively bulky, especially considering that they are attached to the silicate network. In addition, the Na^+ cations should interact relatively weakly with the phosphonate groups. Both these features should improve the mobility of the Na^+ cations. Another factor is the mobility of the polymer itself, which depends on the mobility of the amorphous phase characterized by T_g and the amount of crystalline phase. Normally, PEGs with molecular weights below 800 are liquids at room temperature,[63] while some melting may be observed in the range of 20−25 °C for PEG with an approximate molecular weight of 600.[64] The representative DSC traces of the composite SIC (T-G-S-PEG-3-1) and PEG with a molecular weight of 600 are presented in Figure 3. The DSC trace of PEG shows two transitions: a very weak glass transition at T_g of about −68 °C and melting with the center of gravity of 19 °C. The ΔH of the melting is 68.3 J/g. Using the formula $X_c = \Delta H_m/\Delta H_m^0$ where X_c is the degree of crystallinity, ΔH_m^0 is the heat of melting of 100% crystalline PEO (196.8 J/g), and ΔH_m is the heat of melting of the sample studied,[65] one can estimate the degree of crystallinity of PEG used in this work as 35%. The DSC traces of the composite SICs show, in addition to a pronounced glass transition and melting, a crystallization event as well. The T_g values and crystallization and melting events for the materials under study are presented in Table 1. From these data, one can see that all these materials have low T_g, at about −70 °C, indicating no decrease of PEG mobility compared to a homopolymer. Above the glass transition, SPE

(59) Göltner, C. G.; Henke, S.; Weissenberger, M. C.; Antonietti, M. *Angew. Chem., Int. Ed.* **1998**, *37*, 613−616.
(60) Göltner, C. G.; Berton, B.; Kramer, E.; Antonietti, M. *Adv. Mater.* **1999**, *11*, 395−398.
(61) Finnefrock, A. C.; Ulrich, R.; Du Chesne, A.; Honeker, C. C.; Schumacher, K.; Unger, K. K.; Gruner, S. M.; Wiesner, U. *Angew. Chem., Int. Ed.* **2001**, *40*, 1208−1211.
(62) Simon, P. F. W.; Ulrich, R.; Spies, H. W.; Wiesner, U. *Chem. Mater.* **2002**, *13*, 3464−3486.
(63) Salamone, J. C., Ed. *Polymeric Materials Encyclopedia*; CRC Press: Boca Raton, FL, New York, 1996; Vol. 8.
(64) Mark, H. F., Bikales, N. M., Overberger, C. G., Menges, G., Eds. *Encyclopedia of Polymer Science and Engineering*; John Wiley and Sons: New York, 1986; Vol. 6.
(65) Pielichowski, K.; Flejtuch, K. *Polym. Adv. Technol.* **2002**, *13*, 690−696.

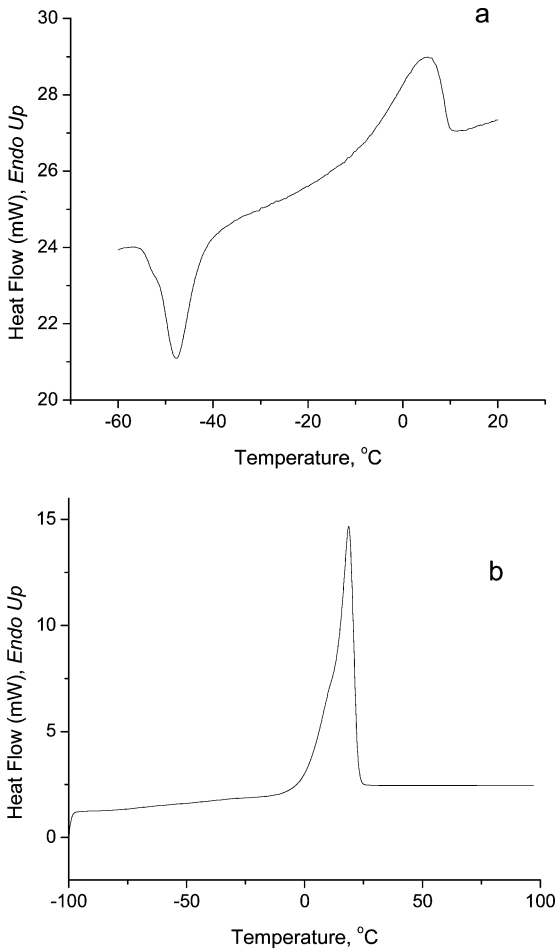

Figure 3. DSC traces of (a) single-ion conductor T-G-S-PEG-3-1 (see Table 1 for values) and (b) PEG.

films first show crystallization (at about −50 °C) and then melting (at about 1−4 °C). A similar DSC trace was reported in ref 66 for oligoethylene glycol placed in the confined environment of a porous layer-by-layer (LBL) polyelectrolyte thin film. Assuming that melting in SIC comes exclusively from the PEG crystalline regions and taking into account that SIC contains only 45% PEG, we can estimate the degree of crystallinity of PEG in SICs as about 32% of 100% crystalline PEG, revealing almost no suppression of PEG crystallization in these composite SPEs. On the other hand, a marked glass transition in all SIC samples reveals that amorphous and crystalline areas are well-separated. Evidently, the heating rate of 10 deg/min is sufficiently slow to observe crystallization of the SIC samples, while the same rate applied to PEG is too fast for observation of PEG crystallization. We conjecture that the presence of OIC particles in SICs aids in enhancing nucleation kinetics due to extensive interface between the SIC components. Depression of the melting point is consistent with development of extensive interfaces[67] in this system, similar to reported confinement effects.[68] The XRD profile of this material presented in Figure 4 shows that at room temperature the material is fully amorphous.

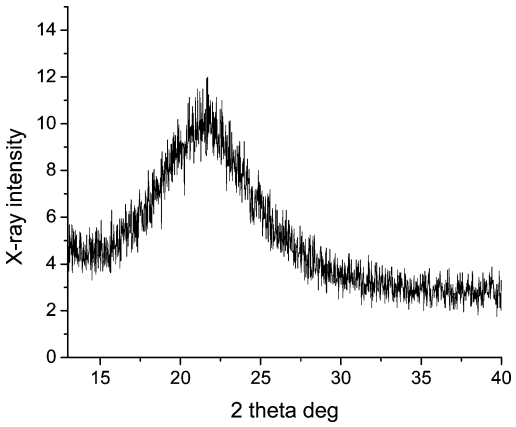

Figure 4. XRD profile of T-G-S-PEG-3-1.

Electrochemical Properties. From the data presented in Table 1, one can see that, for the majority of the samples, the conductivity of the T-G-S-PEG films at room temperature is about 10^{-5} S cm^{-1}, which is a respectable value for single-ion conductors. This result is obtained if the SPE films are made from sol-containing (transparent) reaction solutions before the extensive gel formation takes place (before the reaction solution becomes turbid). The TEM image of such a sample, T-G-S-PEG-3-2, after calcination (Figure 2b) shows comparatively large porous particles, which is a striking contrast with the silicate particles featured in Figure 2a. The decrease of conductivity in the case of large OIC particles may be attributed to the fact that the lower fraction of the SPMP tails is located at the particle surface (despite the silicate particle porosity), and thus fewer cations are exposed to PEG and can participate in the conduction process. This is consistent with the fact that a decrease of conductivity also occurs when the molar ratio of Na to PEG decreases to 1:14, revealing insufficient concentration of cations in PEG. It is noteworthy that for composite materials developed by us earlier and based on Li triflate,[31,36,37] the optimal Li-to-PEG ratio was 1 to 14, because in those materials lithium triflate was solely located within PEO or at the PEO/OIC interface and thus was available for conduction.

As seen from Table 1, the transference number for the majority of the samples is 0.7, i.e., lower than the unity value expected for a SIC. The lower value could be caused by the presence of some other mobile ions in the system along with Na^+ cations. Because SPMP may contain about 5% free sodium phosphate, this might reduce the transference numbers to ∼0.9, but not to 0.7. Another possible source of mobile ions is an anion from noncondensed SPMP precursor: the SPMP reactivity is much lower than that of GLYMO and TMOS, and one might expect incomplete condensation. However, the ^{29}Si CP MAS NMR spectra discussed above unambiguously prove a high degree of condensation of all silanes including SPMP and an absence of free SPMP in the sample.

An additional factor whose influence might alter the cation transference number is moisture absorbed during handling (for example, taking a sample out of a vacuum oven at 130 °C and removal of the film from the dish carried out under air; the cooling of the sample after 130 °C treatment was

(66) Lowman, G. M.; Tokuhisa, H.; Lutkenhaus, J. L.; Hammond, P. T. *Langmuir* **2004**, *20*, 9791−9795.
(67) Maeda, N.; Christenson, H. K. *Colloids Surf., A* **1999**, *159*, 135−148.
(68) Rault, J. *J. Macromol. Sci.* **2003**, *B42*, 1235−1247.

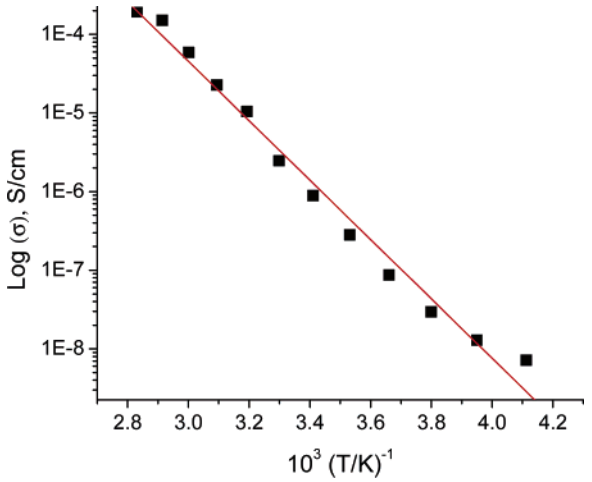

Figure 5. Temperature dependence of conductivity and Arrhenius plot of the T-G-S-PEG-3-1 film with the 33 μm film thickness (where, for example, 1E-4 represents 1×10^{-4}).

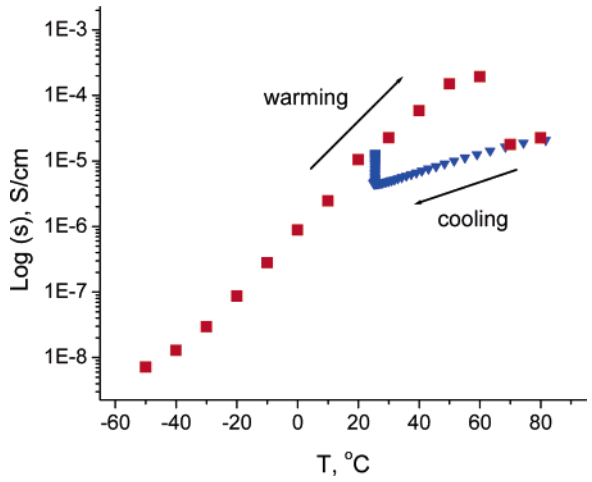

Figure 6. Dependence of conductivity on the thermal history of the T-G-S-PEG-3-1 film with the 33 μm film thickness (where, for example, 1E-3 represents 1×10^{-3}). Red squares show warming, while blue triangles indicate cooling.

carried out in a desiccator). To exclude the moisture influence, we additionally dried the sample T-G-S-PEG-3-1 at 30 °C for 24 h prior to examination. In so doing no changes in glass or melting transitions were detected by DSC measurements. At the same time, this drying resulted in an increase of conductivity by almost an order of magnitude, bringing the conductivity to an exceptionally high (for SIC) value (9.13×10^{-5} S/cm) and an increase of the transference number to 0.9. We think that, in the presence of moisture, Na^+ cations can be hydrated and these hydrated cations, Na^+-$(H_2O)_x$, are responsible for a decrease of the cation transference number. An increase of conductivity may be attributed to a higher mobility of Na^+ compared to bulkier $Na^+(H_2O)_x$. The same drying procedure applied to another sample, T-G-S-PEG-3-3, led to a similar improvement (see Table 1), revealing that this is a common feature of these samples.

We studied the conductivity of T-G-S-PEG-3-1 as a function of temperature with two SPE films with thicknesses of 33 and 165 μm and the dependence of conductivity on thermal history using the experimental protocol described in the Experimental Section. For the 33 μm film, the initial room-temperature conductivity value was 1.4×10^{-5} S/cm (Figure 5). The activation temperature was found to be 8093 K, corresponding to 67 kJ/mol. Another sample in this series (but 165 μm thick) had a room-temperature conductivity of 1.2×10^{-5} S/cm and an activation temperature of 8033 K (also 67 kJ/mol). Evidently, in this thickness range no thickness dependence of conductivity is observed, suggesting homogeneity of the SPE films based on a single ion conductor. This finding is in clear contrast with anisotropic composite SPEs based on aluminosilicate OIC studied by us earlier.[36]

Figure 6 shows dependence of conductivity on the thermal history of T-G-S-PEG-3-1. When warmed (red squares), the conductivity increases fairly rapidly to 60 °C, above which the conductivity progressively drops and stabilizes at 80 °C after being held there for several hours. The frequency dependence of the admittance also changes appropriately (that is, it resembles the admittance measured at a lower temperature with the same bulk conductivity). Upon cooling (blue diamonds), the conductivity decreases monotonically.

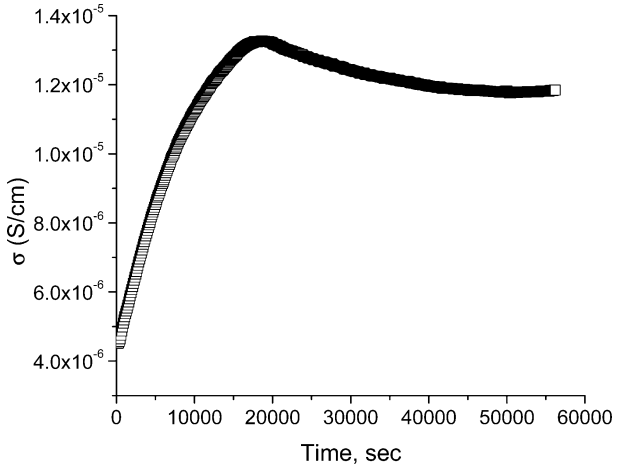

Figure 7. Time dependence of conductivity of the T-G-S-PEG-3-1 film at 25 °C after a cooling−heating cycle.

When the sample is held at 25 °C for 4 days, the conductivity rises to a value close to the original state. However, when the sample cools back to 25 °C, the conductivity first rises dramatically over time and then falls somewhat (Figure 7). The entire cycle—heating, cooling, and annealing—can be repeated on the same sample with similar results.

One possible reason for the drop of conductivity at the temperature above 60 °C could be a differential expansion coefficient between the SPE film and a sputtered gold film, breaking up the sample or at least changing the effectiveness of the contact between the SPE film area and the electrode. However, the time dependence of the effect does not track the time dependence of the temperature changes in the sample; also, such behavior would be unlikely to be repeatable. In addition, the observed change in the frequency dependence of the impedance would not result from a simple change in the effective sample geometry. We believe this behavior should be attributed to a composite nature of these materials.

Conclusion

We synthesized and studied composite SIC based on PEG and OIC formed in situ by sol−gel reaction of three

components: SPMP, GLYMO, and TMOS. TMOS enhances the 3D character of OIC due to four siloxy bonds formed by condensation, GLYMO improves the compatibility of PEG with OIC, and SPMP supplies tethered anions. Altogether they produce OIC as regular particles with a mean diameter of about 15 nm and with a high degree of condensation of siloxy moieties. Adsorption of PEG on the OIC particles does not alter the PEG mobility, while facilitating its crystallization upon cooling. At room temperature the composite materials are fully amorphous.

Variation of the reaction conditions such as the reagent molar ratio, their concentration, the PEG content, and the reaction time shows a weak influence on structure and electrochemical properties of the composite material with two exceptions. Formation of large OIC particles upon progress of condensation and decrease of the sodium fraction below the optimal level lead to a decrease of conductivity by approximately a half-order of magnitude. When the samples contain some moisture, the conductivity measures about 10^{-5} S/cm and the cation transference number does not exceed 0.7 due to formation of $Na^+(H_2O)_x$. When moisture is removed upon drying at 30 °C in a vacuum oven, the conductivity increases by an order of magnitude, while the cation transference number reaches 0.9, demonstrating excellent properties of SICs developed in this work. Variable-temperature conductivity studies show that electrochemical properties of these materials are independent of the SPE film thickness in the range 33−165 μm, yet the conductivity is dependent on the thermal history of the sample.

Acknowledgment. The authors thank NASA for Grant NAG3-2588 for financial support of this project.

CM052195L